GLASS LASER ABLATION-INDUCTIVELY COUPLED PLASMA-MASS SPECTROMETRY ANALYSIS METHODS, PRECISION, AND ACCURACY DATA FOR TEPHRA STUDIES IN ALASKA

Jordan Lubbers, and Matthew Loewen

Techniques and Methods 1

2025
STATE OF ALASKA
DEPARTMENT OF NATURAL RESOURCES
DIVISION OF GEOLOGICAL & GEOPHYSICAL SURVEYS

STATE OF ALASKA
Mike Dunleavy, Governor

DEPARTMENT OF NATURAL RESOURCES
John Boyle, Commissioner

DIVISION OF GEOLOGICAL & GEOPHYSICAL SURVEYS
Melanie Werdon, State Geologist & Director

Publications produced by the Division of Geological & Geophysical Surveys are available to download from the DGGS website (dggs.alaska.gov). Publications on hard-copy or digital media can be examined or purchased in the Fairbanks office:

Alaska Division of Geological & Geophysical Surveys (DGGS)
3354 College Road | Fairbanks, Alaska 99709-3707
Phone: 907.451.5010 | Fax 907.451.5050
dggspubs@alaska.gov | dggs.alaska.gov

DGGS publications are also available at:

Alaska State Library, Historical
Collections & Talking Book Center
395 Whittier Street
Juneau, Alaska 99801

Alaska Resource Library and
Information Services (ARLIS)
3150 C Street, Suite 100
Anchorage, Alaska 99503

Suggested citation:
Lubbers, Jordan, and Loewen, Matthew, 2025, Glass laser ablation-inductively coupled plasma-mass spectrometry analysis methods, precision, and accuracy data for tephra studies in Alaska: Alaska Division of Geological & Geophysical Surveys Techniques and Methods 1, 20 p. https://doi.org/10.14509/31471

GLASS LASER ABLATION-INDUCTIVELY COUPLED PLASMA-MASS SPECTROMETRY ANALYSIS METHODS, PRECISION, AND ACCURACY DATA FOR TEPHRA STUDIES IN ALASKA

Jordan Lubbers[1], and Matthew Loewen[1]

ABSTRACT

This publication reports the analytical conditions, standard reference material (SRM) results, and preferred post-processing methodologies for laser ablation inductively coupled plasma mass spectrometry (LA-ICP-MS) measurements supporting tephra studies in Alaska between 2018 and 2024. We evaluate the long-term accuracy and precision of our methodologies by comparing our calculated SRM concentrations to the Geological and Environmental Reference Materials database (GeoReM) preferred concentration values for the following SRMs: BCR-2G, BHVO-2G, ATHO-G, NIST-612, GSD-1G, and GSE-1G. We show that our LA-ICP-MS methodologies produce accurate and consistent measurements across numerous analytical sessions, even when instrumentation changed. Overall, these results indicate that Alaska tephra matrix glass measurements, like SRM measurements, are accurate, precise, and comparable between analytical sessions. This work allows us to better correlate tephra units from Alaska volcanoes throughout the Alaska-Aleutian arc, ultimately enhancing our understanding of spatiotemporal patterns of volcanism in the region. This enhanced understanding will aid in refining volcanic hazard classification and response strategies. Future versions of this dataset will provide updates to SRM results or analytical routines for sessions that have transpired since the publishing of this version.

INTRODUCTION

This report and accompanying data files describe the methods, individual secondary standard reference material (SRM) analyses, and summary statistics for SRMs measured during tephra matrix glass laser ablation-inductively coupled plasma-mass spectrometry (LA-ICP-MS) analytical sessions conducted between 2018 and 2024. During this time, consistent LA-ICP-MS analytical setups and data processing routines were employed, although variations did occur, including a transition between two different mass spectrometers and laser ablation systems. The goal of this standardization is to ensure that data from unknown sample analyses is precise and comparable over time and between laboratories. We verify performance through tracking SRMs analyzed over the entire period. As a result, data collected over this period has documented consistency, allowing confident assessment of compositional variation between different volcanoes or eruptive periods. Digital data accompanying this report can be downloaded at doi.org/10.14509/31471.

[1] U.S. Geological Survey, Alaska Volcano Observatory

DELIVERABLES

The accompanying data has the following structure.

- Data Dictionary: List of all other sheet names, column names within the sheet, brief description of each column header, and units for each column where applicable.
- Conditions: Analytical conditions for each unique session (i.e., week-long series of analyses). Uses MethodID column to link to SRM concentrations and SRM accuracies sheets.
- SRM concentrations: Calculated concentrations for all standard reference material (SRM) analyses used in this report.
- SRM accuracies: Calculated accuracies (100*measured/accepted values) for all concentrations.
- SRM accuracy stats: Table of mean accuracy and standard deviation values for each SRM
- BCR-2G accuracy stats: Detailed statistics (count, mean, standard deviation, min, quartiles, max, median, skew, kurtosis) for all BCR-2G accuracy values.
- GSD-1G accuracy stats: Detailed statistics (count, mean, standard deviation, min, quartiles, max, median, skew, kurtosis) for all GSD-1G accuracy values.
- NIST-612 accuracy stats: Detailed statistics (count, mean, standard deviation, min, quartiles, max, median, skew, kurtosis) for all National Institute of Standards and Technology (NIST)-612 accuracy values.
- ATHO-G accuracy stats: Detailed statistics (count, mean, standard deviation, min, quartiles, max, median, skew, kurtosis) for all ATHO-G accuracy values.
- BHVO-2G accuracy stats: Detailed statistics (count, mean, standard deviation, min, quartiles, max, median, skew, kurtosis) for all BHVO-2G accuracy values.
- GEOREM: Table of GeoReM preferred values for all SRMs analyzed in this report used to calculate concentrations.

This approach follows the recommended global tephra community best practice guidelines endorsed by the International Association of Volcanology and Chemistry of the Earth's Interior (IAVCEI) Commission on Tephrochronology (Wallace and others, 2022). In compiling this multi-year SRM dataset, we provide a transparent and complete estimate of the accuracy and/or precision for projects that collect data over multiple years and potentially between different labs/analytical setups. This report complements a similar effort by Loewen and others (2023) to document the electron microprobe method and SRM results.

METHODS

Unknown tephra samples were mounted with epoxy in 25 mm-diameter rounds (hereafter called "round mounts"), progressively polished with diamond grit (to 1 μm) with a finishing polish of either colloidal silica (to 0.05 μm) or alumina suspension (0.1 μm).

Carbon coats, added previously for EPMA analysis, were removed prior to analysis using an alumina suspension polish.

All analyses were performed at the W.M. Keck Collaboratory for Plasma Spectrometry at Oregon State University in Corvallis, Oregon. During the timeframe that this comparison covers, multiple laser ablation–quadrupole mass spectrometer combinations were used, ultimately leading to the analytical conditions outlined in table 1.

Total ablation time for all measurements is approximately 20–30 seconds, excluding a 20–30 second delay prior to ablation that is used to establish mass spectrometer background counts and a 10–30 second washout period following ablation and prior to starting data collection on the next sample. Prior to most analyses (apart from those analyzed in May and October 2022), analyzed spots were cleaned using 2–4 pre-ablation cleaning pulses at a larger diameter spot size.

Table 1. Analytical setup conditions for each week-long session at the OSU Keck Lab. Additional analytical details in a machine-readable data file are available in the Supplementary material.

Experiment Month-Year	Laser System	Quadrupole	Laser Energy ($J \cdot cm^2$)	Spot size (μm)	Laser pulse rate (Hz)	Calibration standard
Jan-2018	Photon Machines Analyte G2	ThermoFisher Scientific X Series 2	7	50	7	GSE-1G
Nov-2018	Photon Machines Analyte G2	ThermoFisher Scientific X Series 2	7	50	7	GSE-1G
Jan-2022	Photon Machines Analyte G2	ThermoFisher Scientific iCAP RQ	5	30	7	GSE-1G
May-2022	Applied Spectra RESOlution SE	ThermoFisher Scientific iCAP RQ	5	24	10	GSE-1G
Oct-2022	Applied Spectra RESOlution SE	ThermoFisher Scientific iCAP RQ	5	24	10	GSE-1G
Oct-2023	Applied Spectra RESOlution SE	ThermoFisher Scientific iCAP RQ	5	24–30	10	GSD-1G
Mar-2024	Applied Spectra RESOlution SE	ThermoFisher Scientific iCAP RQ	5	24	10	GSD-1G

Elemental concentrations for all measurements were calculated from raw signals using the equations outlined in Longerich and others (1996) implemented by the Python package

lasertram (Lubbers, 2024). All analytes are collected using a 10 ms dwell time, and ^{29}Si was used as the internal standard. SiO_2 concentrations used for all SRM measurements are the preferred GeoReM values (Jochum and others, 2007a, version 8). GSE-1G, a synthetic glass doped with ~100s ppm trace elements (Guillong and others, 2005), was used as the primary calibration standard for analyses between 2018 and 2022, and GSD-1G (similar to GSE-1G but doped with ~10s ppm trace elements) was used as the primary calibration standard from 2023 to 2024. We recommend these over the commonly used NIST-612 glass based on the following reasons:

- The GS series of glasses do not have documented heterogeneity (Guillong and others, 2005) for certain trace elements like NIST-610–617 glass standards (Eggins and others, 2002; table 2, fig. 1, app. A).
- The GS series of glasses have a basaltic glass matrix which more similarly matches that of tephra glass. While matrix effects on LA-ICP-MS data reduction are likely to be small due to the use of an internal standard (e.g., Jackson, 2008; Sylvester, 2008), the ratio of a measured concentration to the GeoReM accepted concentration (relative sensitivity factor [RSF]) can be influenced by the matrix of the unknown sample (Kroslakova and Gunther, 2007) and potentially up to 15 percent higher when the matrix of the calibration SRM and unknown material do not match (e.g., NIST-612; Jochum and others, 2007b).
- The absorptivity between the GS glasses is likely more like that of our tephra matrix glasses than NIST-612. This ultimately leads to more accurate concentrations being calculated as more similar particle distributions are generated during ablation between the calibration standard and unknown materials (Jochum and Stoll, 2008).

Table 2. Mean accuracy for all analyte (row)–SRM (column) pairs for all analyses from 2018 to 2024. Accuracy is 100*measured/accepted concentration. Please see the attached data tables for more statistics on each SRM.

Analyte	ATHO-G	BCR-2G	BHVO-2G	GSD-1G	NIST-612
^{7}Li	103	101	100	103	99
^{31}P	142	120	100	171	163
^{43}Ca	103	102	97	97	107
^{45}Sc	186	116	101	105	121
^{47}Ti	100	98	96	104	102
^{51}V	114	103	106	100	106
^{55}Mn	102	102	105	99	107
^{65}Cu	100	86	97	99	102
^{66}Zn	93	120	113	99	99

Analyte	ATHO-G	BCR-2G	BHVO-2G	GSD-1G	NIST-612
^{85}Rb	95	96	94	98	98

Table 3, cont. Mean accuracy for all analyte (column)–SRM pairs for all analyses from 2018 to 2024. Accuracy is 100*measured/accepted concentration. Please see the attached data tables for more statistics on each SRM.

Analyte	ATHO-G	BCR-2G	BHVO-2G	GSD-1G	NIST-612
^{88}Sr	100	98	95	96	107
^{89}Y	102	94	81	92	114
^{90}Zr	105	98	87	97	114
^{93}Nb	93	93	86	97	93
^{133}Cs	96	99	94	100	103
^{137}Ba	101	99	97	100	103
^{139}La	102	101	94	96	110
^{140}Ce	102	97	96	97	106
^{141}Pr	101	97	90	97	109
^{146}Nd	103	98	93	97	109
^{147}Sm	103	97	92	96	108
^{153}Eu	104	99	92	96	110
^{157}Gd	104	99	89	94	118
^{163}Dy	104	96	87	95	111
^{166}Er	110	101	88	98	120
^{172}Yb	100	96	84	94	110
^{178}Hf	102	96	86	96	117
^{181}Ta	90	86	80	94	93
^{208}Pb	91	97	103	97	103
^{232}Th	102	98	84	99	110
^{238}U	97	99	100	100	104

ACCURACY AND PRECISION

For all 2018 LA-ICP-MS analytical sessions, SRM duplicate blocks of BHVO-2G, BCR-2G, and NIST-612 were run at the beginning and end. While not included in this report, ATHO-G was run as an SRM under similar analytical conditions and instrument setup as our 2018 work in Loewen and Bindeman (2015). In addition to these SRMs, potential primary standards (hereafter referred to as calibration standards), GSD-1G, and GSE-1G were run approximately every 15 minutes. For 2022 analyses, SRM duplicate blocks were GSD-1G, GSE-1G, BCR-2G, ATHO-G, and NIST-612. Calibration standards GSD-1G and GSE-1G were similarly run approximately every 15 minutes. Calibration standards run in this fashion allow us to monitor for any potential drift in the analytical signal, and the SRM blocks allow us to monitor the quality (i.e., accuracy and precision) of our unknown samples. In 2023, SRM duplicate blocks included BCR-2G and BHVO-2G. In 2024, SRM duplicate blocks included ATHO-G as well as SRMs included in the 2023 blocks. For both 2023 and 2024, calibration standard GSD-1G was run approximately every 15 minutes, or after every ~10 unknown points, but GSE-1G was omitted.

We report summary accuracy and precision of all SRMs in table 2 and figure 1. Additional summary statistics (i.e., median, quartile ranges, skew, and kurtosis) can be found in the SRM-named sheets in the supplementary data tables. Accuracy is reported as 100*measured/accepted concentrations, and precision is the standard deviation of all accuracy values for a given SRM. Accepted values for each element are the preferred GeoReM values (Jochum and others, 2007a, supplemental table/file N). Breaking down accuracy and precision values between the different mass spectrometers outlined in table 1 shows no systematic or significant statistical difference (fig. 2), demonstrating that, although analytical equipment has changed, our experiment design and data reduction methodologies are robust and capable of producing precise, accurate, and comparable measurements on the multi-year scale.

We find that analyte relative standard deviations are weakly correlated with concentration (fig. 3). This has been noticed in other studies of LA-ICP-MS SRM measurements (e.g., Jochum and others, 2006). An exception to this is phosphorus. When processed using GSE-1G as a calibration standard, it has large, ~20–50 percent, relative standard deviation (RSD) values. These values drop appreciably when data are processed using GSD-1G as a calibration standard (fig. 4), suggesting that the low concentration–high standard deviation phosphorus values in GSE-1G (70 ± 20 ppm vs. 860 ± 160 ppm in GSD-1G), when combined with the high mass 31 background values in the mass spectrometer, create a low signal-to-noise ratio that makes quantifying accurate and precise concentrations challenging. We find that across all standards, this is the only analyte distribution that changes significantly when processed using GSD-1G as a calibration standard (fig. 4).

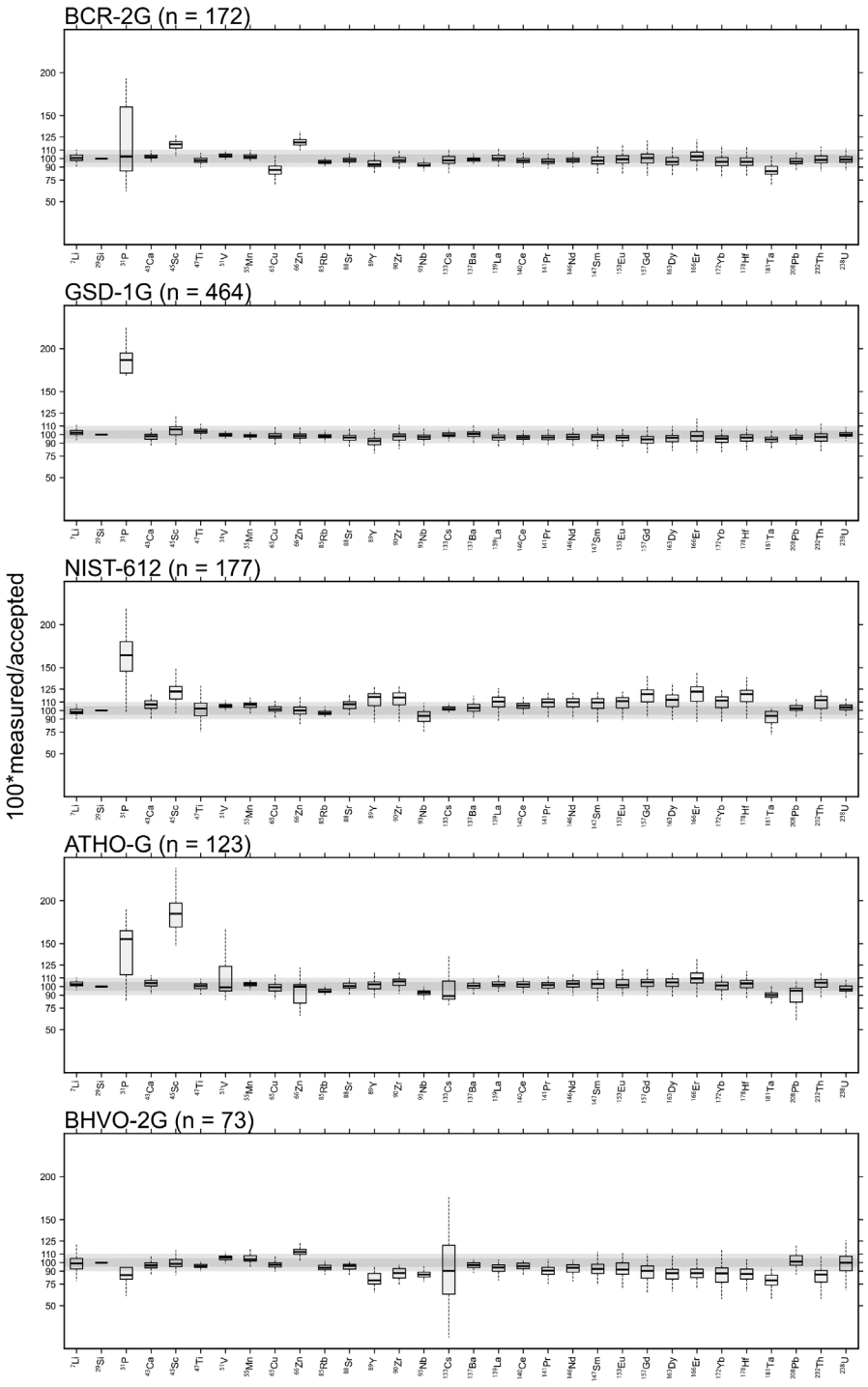

Figure 1. Box and whisker plots of accuracy values for all measurements of a given analyte–SRM pair for all analyses from 2018 to 2024. The number of measurements of each SRM is found in the upper left title of each subplot next to the SRM name. Boxes range from the 25th percentile (Q_1) to the 75th percentile (Q_3) of the data distribution; the whiskers extend to 1.5 * (Q_3–Q_1) from each edge of the box, and the line in the middle of the box represents the distribution median. Analyses determined to be outliers are those that lie outside the whiskers and are not shown here. Overall we see that, with the exception of phosphorus, at least one SRM is reproducing an analyte's concentration to within 5 percent of the GeoReM preferred values.

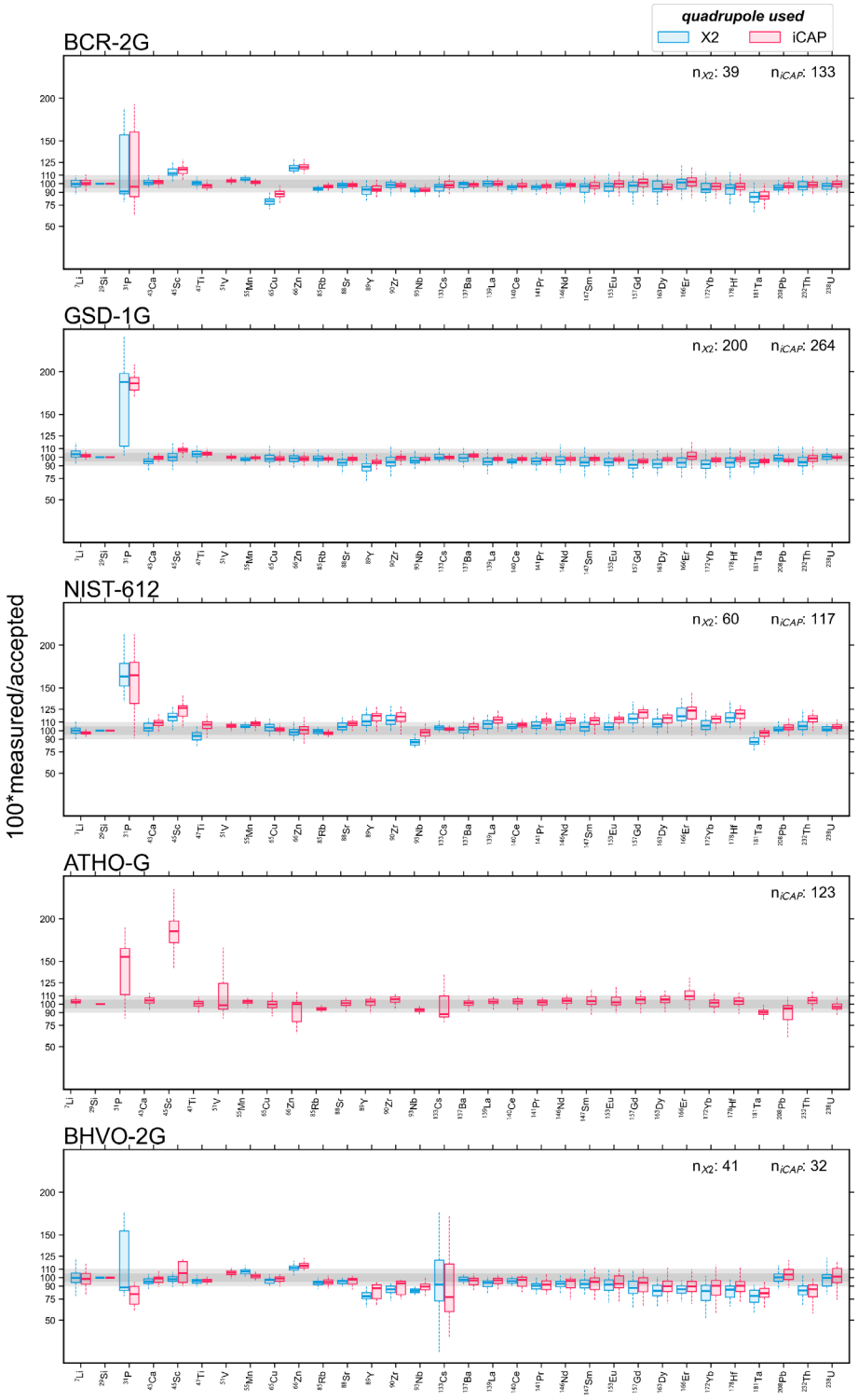

Figure 2. Box and whisker plots of accuracy values for all measurements of a given analyte–SRM pair from 2018 to 2024, this time split by which quadrupole mass spectrometer (e.g., table 1) they were measured with. The number of analyses for each SRM–quadrupole pair is annotated in the upper right. We show here that the use of different mass spectrometers does not influence the median value of our accuracies (and by proxy concentrations) for any analytes, with the exception of phosphorus in GSD-1G and BHVO-2G.

DISCUSSION

Our SRM results from the previous five years demonstrate excellent reproducibility and accuracy following our LA-ICP-MS procedure with concentrations generally within 10 percent of accepted values and reproducibility better than 10 percent (tables 2 and 3). Using GSD-1G as a calibration standard results in similar accuracies and precisions but also gives usable quantitative data for phosphorus from LA-ICP-MS analyses; therefore, we switched to GSD-1G as the preferred calibration standard in all analyses beginning in October 2023. Furthermore, as mentioned above, in using GSD-1G as our calibration standard, we continue to avoid potential heterogeneity and matrix issues observed in other calibration standards such as NIST-612. Because of the close agreement in GSD-1G and GSE-1G-derived concentrations (fig. 4), apart from phosphorus, all previously collected data does not need to be corrected in any way, and all future data collected will continue to be directly comparable, a key component for tephra correlation and petrologic studies (e.g., Lowe and others, 2017).

Our results also indicate there is a limit to the precision of LA-ICP-MS-determined values with our analytical methodology and ones common to other tephra/petrologic studies (~2–3 percent; fig. 3). Our findings are similar to the results of other studies (Jochum and others, 2006). Unlike electron probe data that has uncertainties that are strongly anti-correlated with the concentration of an analyte (e.g., Loewen and others, 2023), LA-ICP-MS relative standard deviations weakly decrease with increasing concentration and then plateau around the 2–3 percent range, pending the SRM being analyzed (fig. 3). This implies a few things, namely: (1) when processing data, individual analysis concentrations that have relative uncertainties less than this are likely underestimating the true precision of that measurement; (2) when comparing datasets, differences less than this threshold cannot be statistically resolved; and (3) there are additional sources of uncertainty in LA-ICP-MS analyses that are not purely related to mass spectrometer counting statistics that likely originate from heterogeneities in other factors such as standard reference materials propagating through data reduction calculations, downhole fractionation, or matrix effects producing variable ablation yields and/or particle size distributions.

Further SRM results will be reported in subsequent versions of this report. In documenting, inspecting, and maintaining a long-term record of SRM results, we hope to identify potential systematic changes that may require correction such that unknown (e.g., tephra matrix glass) analyses are always comparable between studies. As all tephra matrix glass analyses will be stored in the Geologic Database of Information on Volcanoes in Alaska (Cameron and others, 2019; 2022), if any systematic change found in the inspection of our SRM data needs to be applied to previously reported analyses, these adjustments will be made to the analyses in the database in a similar fashion to those made to bulk-rock trace element data (Nye and others, 2018).

Table 4. Standard deviation for all analyte (row)–SRM (column) pairs for analyses from 2018 to 2024. Please see the attached data tables for more statistics on each SRM.

Analyte	ATHO-G	BCR-2G	BHVO-2G	GSD-1G	NIST-612
^{7}Li	3.7	5.1	11.3	4.1	4.0
^{31}P	29.5	39.3	34.2	40.2	40.2
^{43}Ca	7.0	3.8	4.1	4.3	6.1
^{45}Sc	24.1	7.8	9.2	7.0	9.3
^{47}Ti	3.6	3.8	3.8	3.7	9.7
^{51}V	30.5	2.6	3.4	2.3	3.7
^{55}Mn	3.4	2.9	4.2	2.4	3.5
^{65}Cu	7.0	6.3	4.4	4.7	4.1
^{66}Zn	12.2	4.1	4.8	4.3	6.8
^{85}Rb	2.6	2.8	3.7	3.5	2.9
^{88}Sr	6.0	3.7	4.2	4.6	5.5
^{89}Y	5.7	5.3	7.5	5.8	8.5
^{90}Zr	5.0	4.8	6.7	6.2	8.6
^{93}Nb	3.3	3.8	4.7	3.8	7.4
^{133}Cs	15.8	6.2	38.5	3.4	2.8
^{137}Ba	5.2	3.6	4.6	4.7	5.7
^{139}La	5.8	4.4	5.5	4.7	7.0
^{140}Ce	4.7	3.7	4.4	3.5	4.2
^{141}Pr	5.4	4.2	5.9	4.3	6.0
^{146}Nd	5.6	5.2	6.3	5.1	6.8
^{147}Sm	7.8	7.8	9.7	5.6	7.7
^{153}Eu	8.6	7.4	9.2	4.7	7.0
^{157}Gd	6.8	7.8	10.5	6.0	8.7

Table 5, cont. Standard deviation for all analyte (row)–SRM (column) pairs for analyses from 2018 to 2024. Please see the attached data tables for more statistics on each SRM.

Analyte	ATHO-G	BCR-2G	BHVO-2G	GSD-1G	NIST-612
^{163}Dy	6.6	6.9	9.6	6.1	8.4
^{166}Er	10.0	8.4	9.8	8.1	11.7
^{172}Yb	7.1	8.3	14.1	6.0	8.4
^{178}Hf	7.0	8.2	9.6	6.3	8.9
^{181}Ta	4.9	8.6	9.3	4.9	7.4
^{208}Pb	10.9	4.4	10.3	4.3	4.2
^{232}Th	8.8	7.4	10.6	16.0	8.3
^{238}U	4.6	5.5	12.9	3.4	3.7

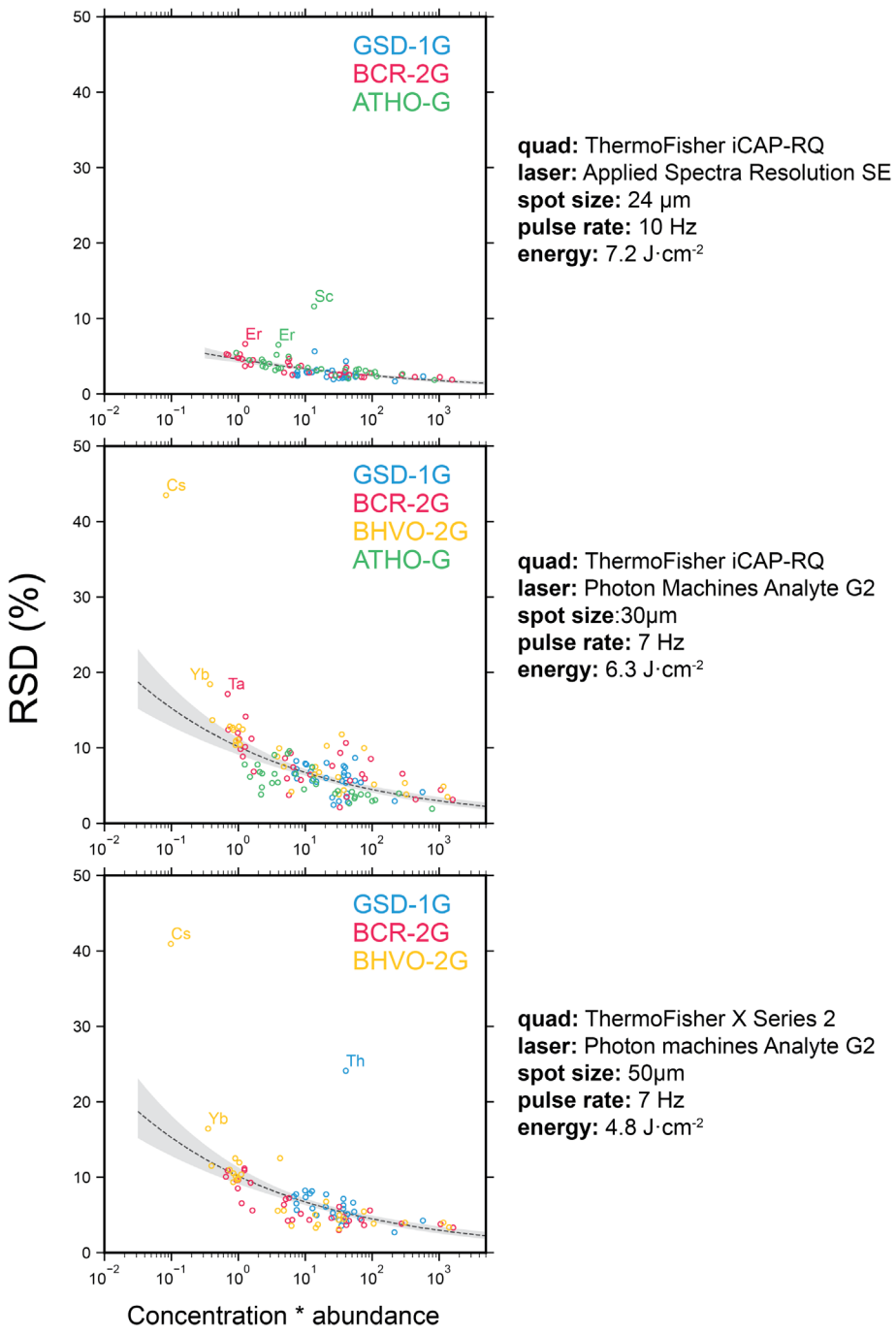

Figure 3. Plots of relative standard deviation (RSD) versus concentration * analyte isotopic abundance showing the relationship between an analyte's uncertainty and its overall abundance in SRMs from our dataset. Here, RSD is the relative standard deviation of the distribution for a given analyte–SRM pair and is effectively a proxy for precision. We see that there is a weakly log-linear negative correlation between an analyte's abundance and its precision; however, at $>\sim 10^2$ concentration * abundance values, the RSD plateaus and does not improve with increasing values, suggesting there is a finite limit to precision in our analytical setup. Black dashed lines and gray regions are regression mean and confidence intervals, respectively, from ordinary least squares regression in log-space: ln(RSD) = m*ln(concentration) + b. This is

displayed only to demonstrate that the weak log-linear negative correlation between RSD and concentration in LA-ICP-MS data is not simply qualitative.

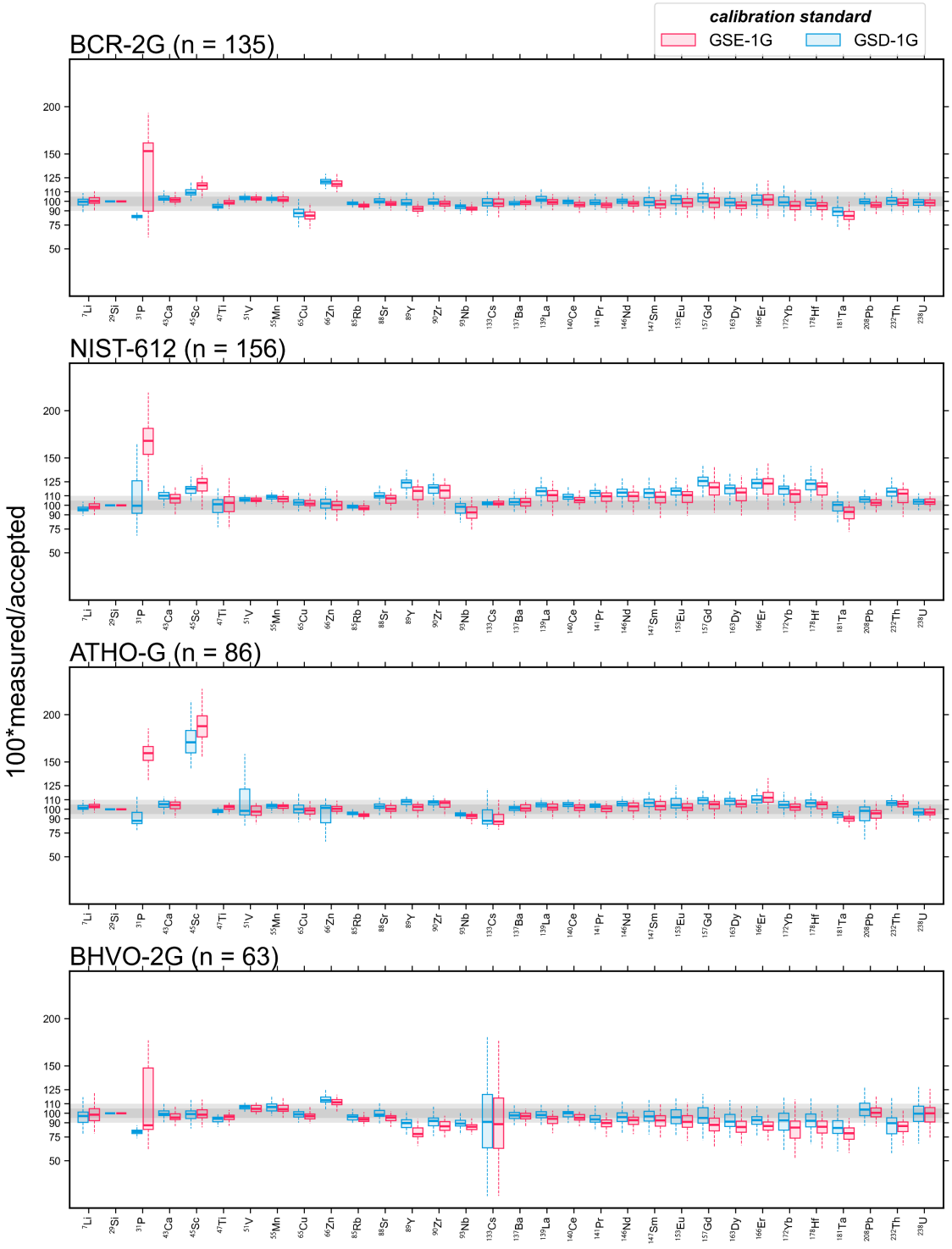

Figure 4. Box and whisker plots of accuracy values for all measurements of a given analyte–SRM pair for analyses from 2018 to 2022, this time split by whether or not they were processed using GSD-1G (blue) or GSE-1G (red) as the calibration standard. We show here that, with the exception of phosphorus, changes in median accuracy (and by proxy, concentrations) are minimal. This validates our change to using GSD-1G as a calibration standard from 2023 onwards.

ACKNOWLEDGMENTS

We would like to acknowledge and express our gratitude to Adam Kent, Chris Russo, Andy Ungerer, and Chuck Lewis for their mentorship and numerous discussions about LA-ICP-MS methodologies over the years. This article has been peer-reviewed and approved for publication consistent with USGS Fundamental Science Practices (pubs.usgs.gov/circ/1367). We appreciate reviews provided by Chris Russo and Jay Thompson and metadata review by Simone Montayne. Any use of trade, firm, or product names is for descriptive purposes only and does not imply endorsement by the U.S. Government.

REFERENCES

Cameron, C.E., Crass, S.W., and AVO Staff, eds., 2022, Geologic Database of Information on Volcanoes in Alaska (GeoDIVA): Alaska Division of Geological & Geophysical Surveys Digital Data Series 20. https://doi.org/10.14509/30901

Cameron, C.E., Mulliken, K.M., Crass, S.W., Schaefer, J.R., and Wallace, K.L., 2019, Alaska Volcano Observatory geochemical database, version 2: Alaska Division of Geological & Geophysical Surveys Digital Data Series 8 v. 2, 22 p. https://doi.org/10.14509/30058

Eggins, S.M., and Shelley, J.M.G., 2002, Compositional heterogeneity in NIST SRM 610-617 glasses: Geostandards Newsletter, v. 26, no. 3, p. 269–286. https://doi.org/10.1111/j.1751-908X.2002.tb00634.x

Guillong, Marcel, Hametner, Kathrin, Reusser, Eric, Wilson, S.A., and Günther, Detlef, 2005, Preliminary characterization of new glass reference materials (GSA-1G, GSC-1G, GSD-1G, GSE-1G) by laser ablation-inductively coupled plasma-mass spectrometry using 193 nm, 213 nm and 266 nm wavelengths: Geostandards and Geoanalytical Research, v. 26, no. 3, p. 315–331. https://doi.org/10.1111/j.1751-908X.2005.tb00903.x

Jackson, S.E., 2008, Calibration strategies for elemental analysis by LA-ICP-MS, *in* Sylvester, P.J., ed., Laser ablation ICP-MS in the earth sciences: Current practices and outstanding issues: Mineralogical Association of Canada Short Course Series, v. 40, p. 169–188.

Jochum, K.P., Nohl, Uwe, Herwig, Kirstin, Lammel, Esin, Stoll, Brigitte, and Hofmann, A.W., 2007a, GeoReM: A new geochemical database for reference materials and isotopic standards: Geostandards and Geoanalytical Research, v. 29, no. 3, p. 333–338. https://doi.org/10.1111/j.1751-908X.2005.tb00904.x

Jochum, K.P., and Stoll, Brigitte, 2008, Reference materials for elemental and isotopic analyses by LA-(MC)-ICP-MS: Successes and outstanding needs, *in* Sylvester, P.J., ed., Laser ablation ICP-MS in the earth sciences: Current practices and outstanding issues: Mineralogical Association of Canada Short Course Series, v. 40, p. 147–168.

Jochum, K.P., Stoll, Brigitte, Herwig, Kirstin, Willbold, Matthias, Hofmann, A.W., Amini, Marghaleray, ...and Woodhead, J.D., 2006, MPI-DING reference glasses for in situ microanalysis: New reference values for element concentrations and isotope ratios: Geochemistry, Geophysics, Geosystems, v. 7, no. 2, 44 p. https://doi.org/10.1029/2005GC001060

Jochum, K.P., Stoll, Brigitte, Herwig, Kirstin, and Willibold, Matthias, 2007b, Validation of LA-ICP-MS trace element analysis of geological glasses using a new solid-state 193 nm Nd:YAG laser and matrix matched calibration: Journal of Analytical Atomic Spectrometry, v. 22, p. 112–121. https://doi.org/10.1039/B609547J

Kroslakova, Ivana, and Günther, Detlef, 2007, Elemental fractionation in laser ablation-inductively coupled plasma-mass spectrometry: evidence for matrix effects in the ICP during ablation of a silicate glass: Journal of Analytical Atomic Spectrometry, v. 22, no. 1, p. 51–62. https://doi.org/10.1039/B606522H

Loewen, M.W., Wallace, K.L., Lubbers, Jordan, Ruth, Dawn, Izbekov, P.E., Larsen, J.F., and Graham, Nathan, 2023, Glass electron microprobe analyses methods, precision and accuracy for tephra studies in Alaska: Alaska Division of Geological & Geophysical Surveys Miscellaneous Publication 174, 22 p. https://doi.org/10.14509/31045

Loewen, M.W., and Bindeman, I.N., 2015, Oxygen isotope and trace element evidence for three-stage petrogenesis of the youngest episode (260–79 ka) of Yellowstone rhyolitic volcanism: Contributions to Mineralogy and Petrology, v. 170, no. 1–25. https://doi.org/10.1007/s00410-015-1189-5

Lubbers, Jordan, 2024, lasertram – Laser Time Resolved Analysis Module (Version 1.0.0): U.S. Geological Survey Software Release. https://doi.org/10.5066/P1DZUR3Z

Longerich, H.P., Jackson, S.E., and Günther, Detlef, 1996, Inter-laboratory note. Laser ablation inductively coupled plasma mass spectrometric transient signal data acquisition and analyte concentration calculation: Journal of analytical atomic spectrometry, v. 11, no. 9, p. 899–904. https://doi.org/10.1039/JA9961100899

Lowe, D.J., Pearce, N.J.G., Jorgensen, M.A., Kuehn, S.C., Tryon, C.A., and Hayward, C.L., 2017, Correlating tephras and cryptotephras using glass compositional analyses and numerical and statistical methods: Review and evaluation: Quaternary Science Reviews 175, p. 1–44. http://dx.doi.org/10.1016/j.quascirev.2017.08.003

Nye, C.J., Begét, J.E., Layer, P.W., Mangan, M.T., McConnell, V.S., McGimsey, R.G., Miller, T.P., Moore, R.B., and Stelling, P.L., 2018, Geochemistry of some Quaternary lavas from the Aleutian Arc and Mt. Wrangell: Alaska Division of Geological & Geophysical Surveys Raw Data File 2018-1, 29 p. https://doi.org/10.14509/29843

Sylvester, P.J., 2008, Matrix effects in laser ablation ICP-MS, *in* Sylvester, P.J., ed., Laser ablation ICP-MS in the earth sciences: Current practices and outstanding issues: Mineralogical Association of Canada Short Course Series, v. 40, p. 67–92.

Wallace, K.L., Bursik, M.I., Kuehn, Stephen, Kurbatov, A.V., Abbott, Peter, Bonadonna, Costanza, Cashman, Katharine, Davies, S.M., Jensen, Britta, Lane, Christine, Plunkett, Gill, Smith, V.C., Tomlinson, Emma, Thordarsson, Thor, and Walker, J.D., 2022, Community established best practice recommendations for tephra studies—from collection through analysis: Scientific Data, v. 9, p. 447. https://doi.org/10.1038/s41597-022-01515-y

APPENDIX A: TIMESERIES BOXPLOTS

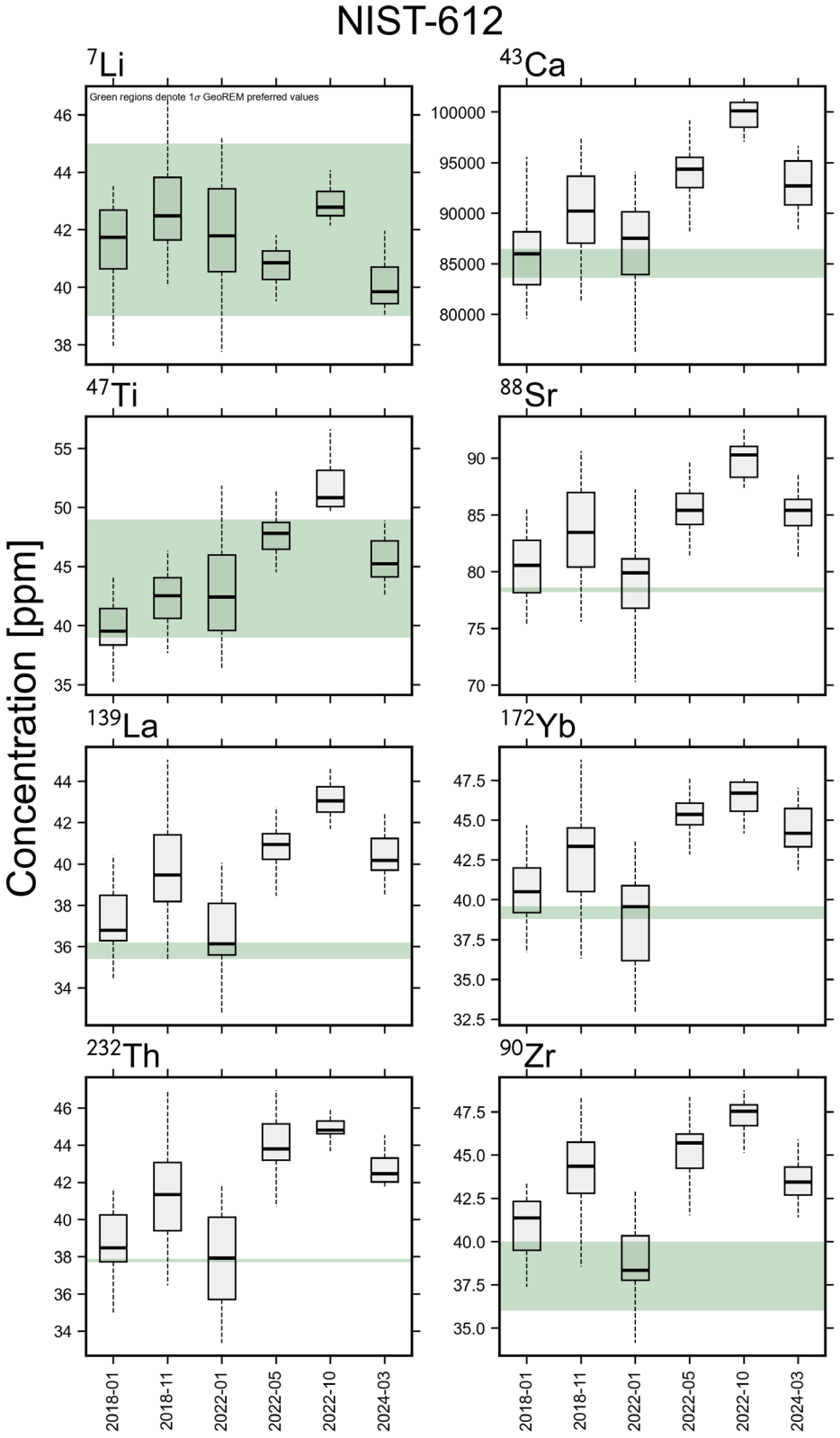

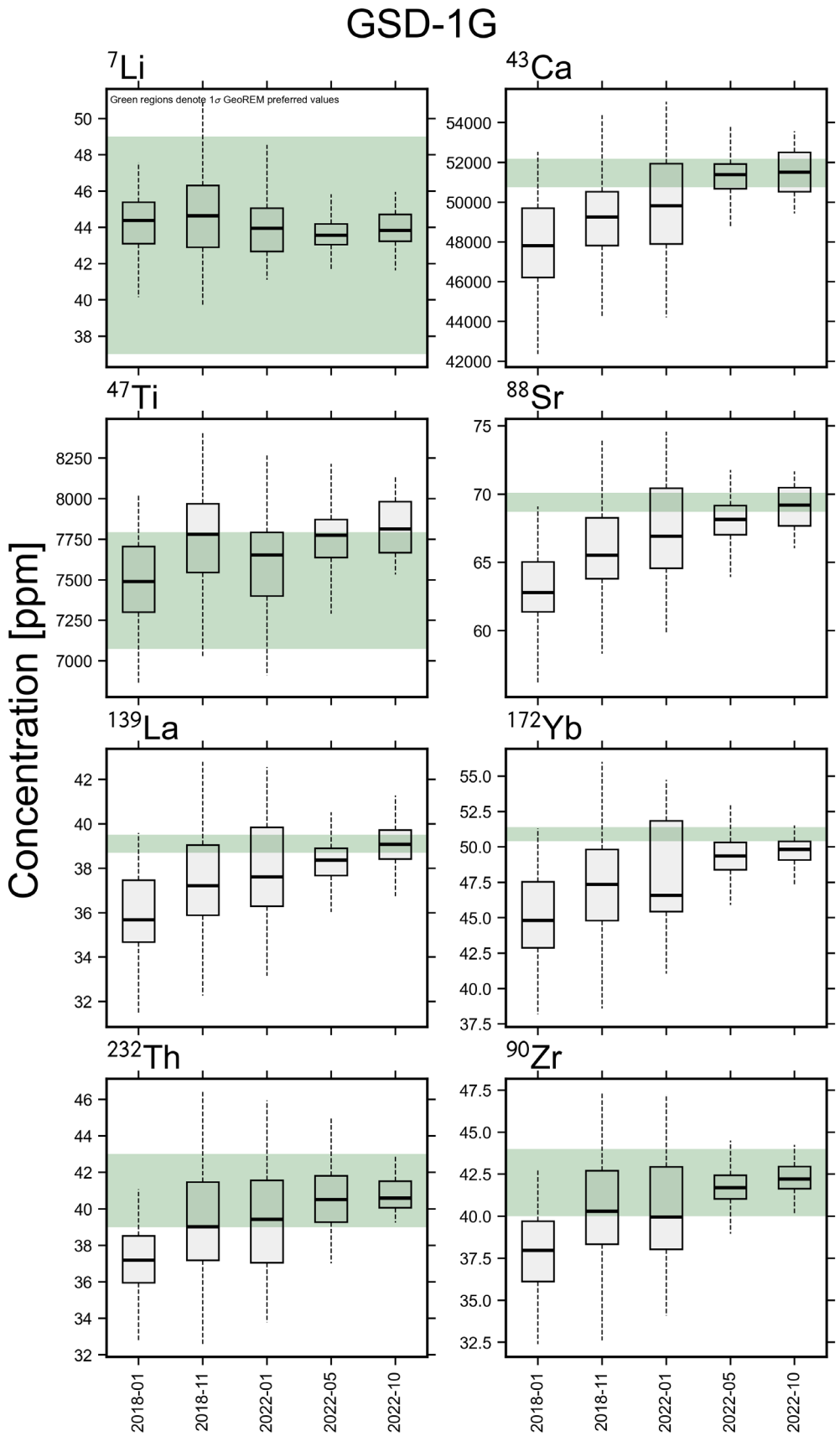
GSD-1G
^{7}Li
Green regions denote 1σ GeoREM preferred values
^{43}Ca
^{47}Ti
^{88}Sr
^{139}La
^{172}Yb
^{232}Th
^{90}Zr
Concentration [ppm]
2018-01
2018-11
2022-01
2022-05
2022-10

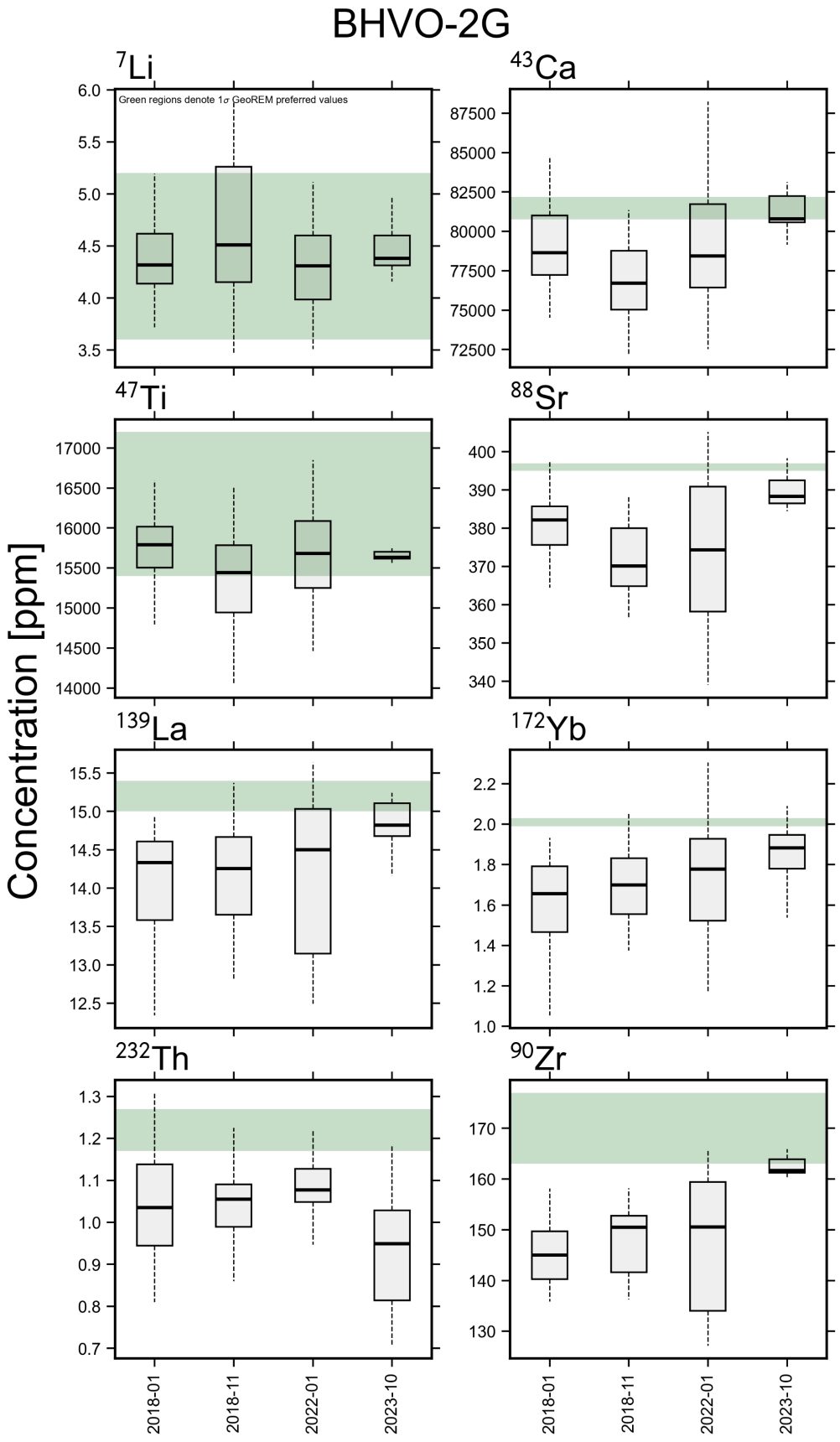
BHVO-2G
7Li
Green regions denote 1σ GeoREM preferred values
43Ca
47Ti
88Sr
139La
172Yb
232Th
90Zr
Concentration [ppm]
2018-01
2018-11
2022-01
2023-10

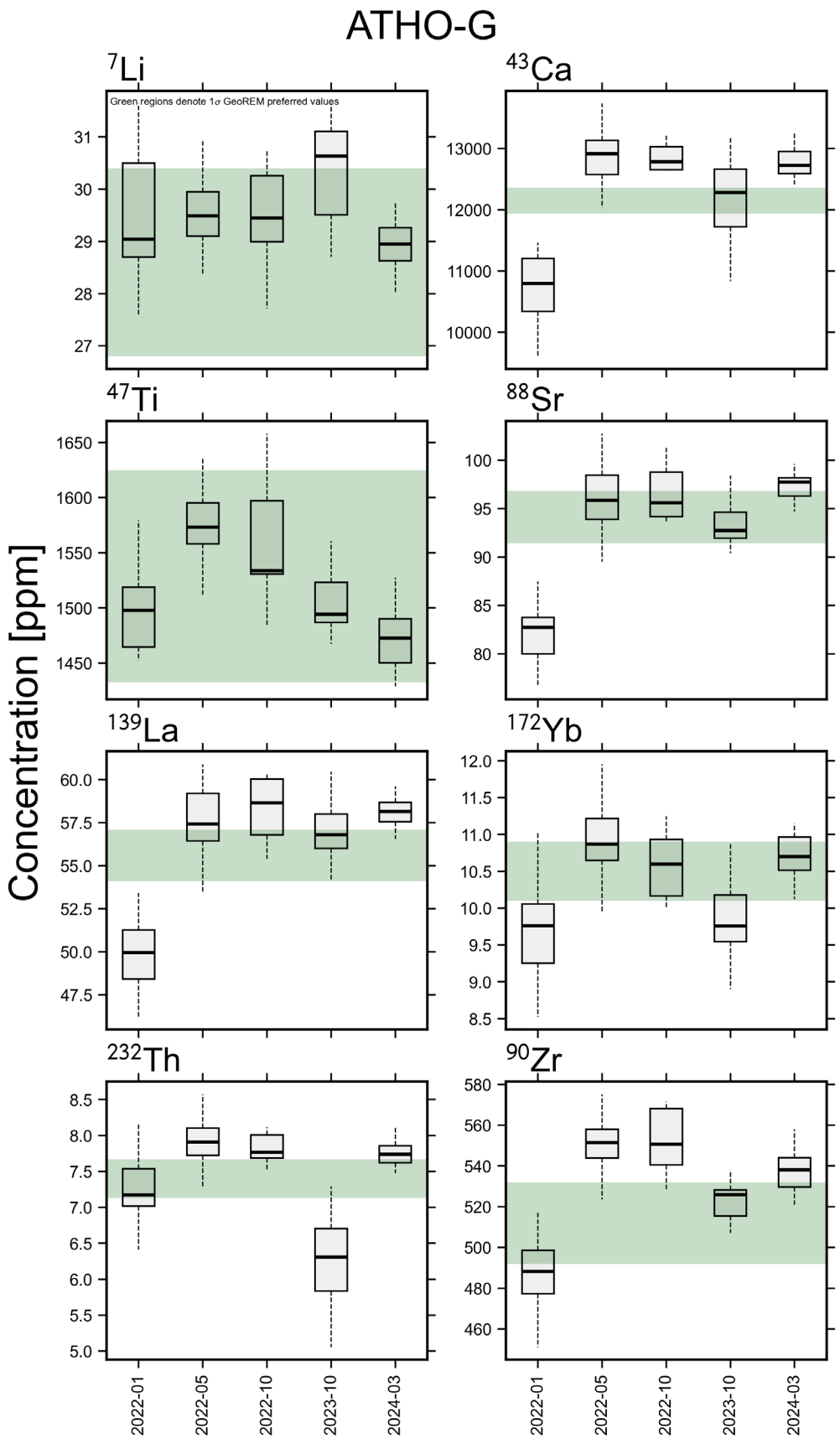
ATHO-G
^{7}Li
Green regions denote 1σ GeoREM preferred values
^{43}Ca
^{47}Ti
^{88}Sr
^{139}La
^{172}Yb
^{232}Th
^{90}Zr
Concentration [ppm]
2022-01
2022-05
2022-10
2023-10
2024-03

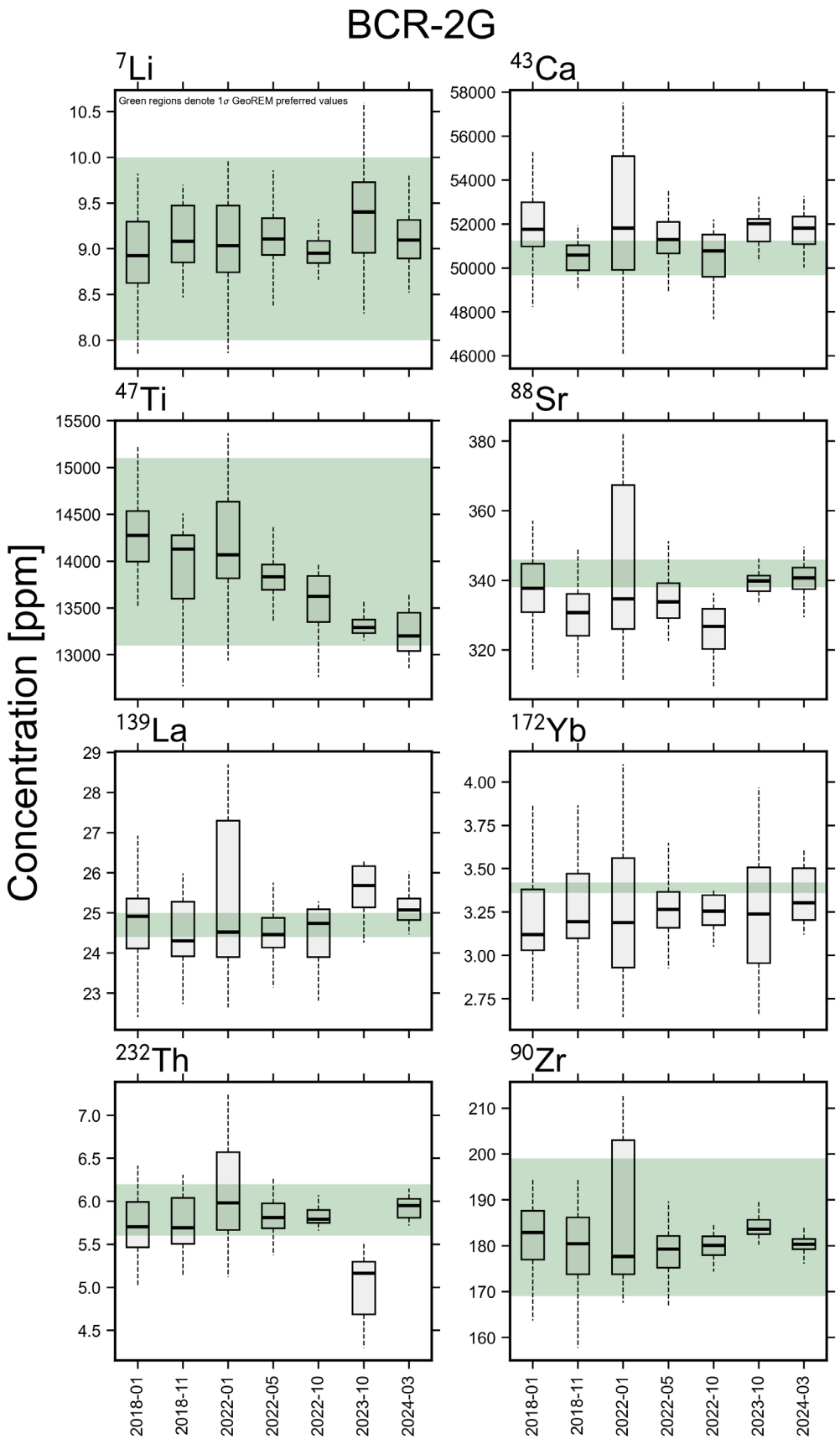
BCR-2G
7Li
Green regions denote 1σ GeoREM preferred values
43Ca
47Ti
88Sr
139La
172Yb
232Th
90Zr
Concentration [ppm]
2018-01
2018-11
2022-01
2022-05
2022-10
2023-10
2024-03